Int. J. Appl. Comput. Math (2022) 8:214
https://doi.org/10.1007/s40819-022-01397-z

ORIGINAL PAPER

Adaptive Technique for Solving 1-D Interface Problems of Fractional Order

Rahma Al-Masaeed[1] · Banan Maayah[1] · Sana Abu-Ghurra[2]

Accepted: 24 June 2022 / Published online: 4 August 2022

Abstract
In this paper, we present a numerical technique for solving 1-D interface problems of fractional order. This technique relies on the reproducing kernel functions and the shooting method. The biggest advantage over the existing standard analytical techniques is overcoming the difficulty arising in calculating complicated terms. Numerical examples are inspected to feature the significant highlights of this technique. Moreover, the solution procedure is simple, more effective and clearer.

Keywords Reproducing kernel method · Shooting method · 1-D interface problems · Caputo fractional derivative operator

Introduction

In the past few decades, many mathematicians and physicists have been concerned with interface problems. It is interesting to explore the ways to solve them. So many numerical methods have been presented to solve these problems.

Interface problems occur in several applications such as dynamical systems [1], fluid mechanics [2], electromagnetic wave propagation [3, 4]. Recently, many researchers have studied numerical methods for solving interface problems such as immersed finite element method [5–7], RKHS methods for 1-D interface problems [8, 9], high-order difference potentials methods [10].

Fractional differential equations (FDEs) occupy a very important area because the important of their applications in many fields of science and engineering [11]. Riemann–Liouville and Caputo were the first to investigate the generalization of ordinary integral and differential operators into fractional derivatives. The fractional-order differential equations offer a logical framework for studying real-world problems such as Rubella disease modal [12], waste water modal [13], economic growth model [14], diffusion processes [15], coronavirus disease and Covid-19 models sense [16, 17], in [18] the authors solve the system of nonlinear

✉ Banan Maayah
b.maayah@ju.edu.jo

1 Department of Mathematics, Faculty of Science, The University of Jordan, Amman 11942, Jordan

2 Department of Mathematics, Faculty of Science, Ajloun National University, Ajloun 26810, Jordan

fractional order PDEs involving of power law kernel using hybrid analytical technique. On the other hand there is some work on a new method for solving fractional PDEs in [19]. In [20–22] some fractional differential equations with decay kernel are disscused. Since it is difficult to find exact solutions in closed forms for most differential equations of fractional order, so approximations and numerical techniques will be used, for more see [23–25].

The hypothesis of the reproducing kernel Hilbert space (RKHS) and its reproducing kernel function (RKF) have important applications in numerical analysis. The researchers applied the RKHS to develop several numerical techniques for solving different types of differential and integral equations, in [26] the authors introduce the solution the ABC- fractional Riccati and Bernoulli equations by using RKHS method. To explain the important of (RKF), (RKHS) you can read more details from Reproducing kernel for solving mixed type singular time-fractional partial integrodifferential equations [27], singularly perturbed boundary value problems with a delay [28], strongly nonlinear Duffing oscillators [29], integrodifferential systems with two-points periodic boundary conditions [30], Bagley–Torvik and Painlevé equations of fractional order [31], fuzzy fractional differential equations in presence of the Atangana–Baleanu–Caputo differential operators [32], time-fractional Tricomi and Keldysh equations [33], ABC–Fractional Volterra integro-differential equations [34], the Atangana–Baleanu fractional Van der Pol damping model [35], time-fractional partial differential equations subject to Neumann boundary conditions [36], singular integral equation with cosecant kernel [37]. In this paper, a new numerical method is proposed for solving 1-D interface problems of fractional order. The method is based on the reproducing kernel functions and the shooting method. In the first step, the boundary value problems are converted to the initial value problem with interface conditions by the shooting method, thereafter the reproducing kernel method is applied for solving the new initial value problems. In addition, we carefully study the effectiveness of this method by solving some numerical examples.

By using a modification of the RKHS method, we try to find an approximate solution to our problem, but we cannot use the RKF-based techniques to solve fractional interface problems directly because of the interface point conditions. Therefore, the main challenge here is to construct an effective and accurate numerical method to solve the 1-D fractional interface problem.

In our work, we consider the following 1-D fractional interface problem

$$\begin{cases} D^{\alpha}\vartheta(\xi) + y_1\vartheta(\xi) = f_1(\xi), \; 0 < \xi < z, \\ D^{\alpha}\vartheta(\xi) + y_2\vartheta(\xi) = f_2(\xi), \; z < \xi < 1 \;\; , 1 < \alpha \le 2, \\ \vartheta(0) = \beta_0, \; \vartheta(1) = \beta_1. \end{cases} \tag{1}$$

and with the interface conditions on z:

$$\begin{cases} \vartheta\left(z^{+}\right) = x_1\vartheta\left(z^{-}\right) + \gamma_0, \\ \vartheta'\left(z^{+}\right) = x_2\vartheta'\left(z^{-}\right) + \gamma_1. \end{cases} \tag{2}$$

where y_1, y_2 are sufficiently smooth functions defined in $(0, z)$, $(z, 1)$ respectively and ϑ is an unknown function that will be determined. The operator D^{α} has the following formula:

$$D^{\alpha}\vartheta(\xi) = \frac{1}{\Gamma(n-\alpha)}\int_0^{\xi}(\xi-\tau)^{(n-1-\alpha)}\vartheta^{(n)}(\tau)d\tau, \qquad 0 < \tau < \xi, \; 1 < \alpha \le 2. \tag{3}$$

is called the Caputo fractional derivative operator of order α of a function $\vartheta(\xi)$.

Let $A(\xi) = \begin{cases} y_1(\xi), & 0 < \xi < z \\ y_2(\xi), & z < \xi < 1. \end{cases}$ and $f(\xi) = \begin{cases} f^1(\xi), & 0 < \xi < z \\ f_2(\xi), & z < \xi < 1. \end{cases}$

Then (1) can be written as

$$\begin{cases} D^{\alpha}\vartheta(\xi) + A(\xi)\vartheta(\xi) = f(\xi), \ \xi \in (0, z) \cup (z, 1), \\ \vartheta(0) = \beta_0, \vartheta(z^+) = x_1\vartheta(z^-) + \gamma_0, \vartheta'(z^+) = x_2\vartheta'(z^-) + \gamma_1, \vartheta(1) = \beta_1. \end{cases} \tag{4}$$

Preliminaries

In this section, we present some basic definitions, results and observations of the shooting method and the reproducing kernel Hilbert spaces that will be required in the sequel to understand the necessary literature and develop our main results.

Shooting Method

In numerical analysis, the shooting method is a technique for converting the boundary value problem to an equivalent initial value problem. Then, an initial value problem is solved via a trial-and-error approach. This technique is called a "shooting" method, by analogizing it to the procedure of shooting an object at a stationary target. Roughly speaking, we shoot out trajectories in different directions until we find a trajectory that has the desired boundary value.

For the utilization of the shooting method: Firstly, we need to reduce the boundary value problem to a system of initial value problems, and we need to assume a guess value at the lower bound of the interval. After these, the solution goes on like the solution of a system of differential equations.

Let us consider a second-order boundary value problem:

$$\begin{cases} \vartheta''(\xi) = f\left(\xi, \vartheta, \vartheta'\right), \ \alpha \le \xi \le \beta \\ \vartheta(\alpha) = \gamma, \qquad \vartheta(\beta) = \eta. \end{cases} \tag{5}$$

At first, we reduce the second-order (BVP) of the equation to a system of a first-order (IVP). The second-order ODE is transformed into a system of two first-order ODEs as:

$$\begin{cases} \frac{d\vartheta}{d\xi} = \vartheta' = x = f_1(\xi, \vartheta, x), \ \vartheta(\alpha) = \gamma, \\ \frac{dx}{d\xi} = \vartheta'' = f_2(\xi, \vartheta, x), \qquad \vartheta(\beta) = \omega. \end{cases} \tag{6}$$

In the wake of choosing the $\hbar$ step size, we use one of the known methods like Euler, Runge–Kutta, etc. to solve these equations. The first numerical result of the BVP is then obtained, which is subject to the first guess value ω. If the solution is close enough to the other bound η, it is valid; otherwise, the method will resume with another guess. Instead of making the third guess arbitrary after the first two, we can utilize interpolation to get the third and if necessary, the subsequent guesses [38]. Note that the interpolation is given by

$$\vartheta(0) = \mathrm{G}_1 + \frac{(\mathrm{G}_2 - \mathrm{G}_1)}{(\mathrm{B}_2 - \mathrm{B}_1)}(\mathrm{D} - \mathrm{B}_1). \tag{7}$$

where: G_1: First guess at the initial slope; G_2: Second guess at the initial slope; B_1: Final result at endpoint (using G_1); B_2: Second result at endpoint (using G_2); D: The desired value at the endpoint.

Reproducing Kernel Hilbert Spaces

We present some fundamental definitions and theorems, which account for a significant part of the study of RKHSs.

Definition 2.2.1 Let M be a nonempty set, the function $\psi : M \times M \to \mathbb{C}$ is called a reproducing kernel function to Hilbert space H iff
(a)

$$\psi(., \xi) \in H, \forall \xi \in M,$$

(b) $\langle \varphi(.), \psi(., \xi)\rangle_H = \varphi(\xi)$ for all $\varphi \in H$ and for all $\xi \in M$.

The second condition is called the reproducing property (the value of the function φ at the point ξ is reproduced by the inner product of φ with $\psi(., \xi)$), where the function ψ is called the reproducing kernel function of H that has some important properties such as being unique, symmetric, and positive definite.

Definition 2.2.2 The function space $W_2^1[a, b]$ is defined by:

$W_2^1[a, b] = \left\{\vartheta | \vartheta \ is\ absolutely\ continuous\ function\ and\ \vartheta' \in L^2[a, b]\right\}$, with the inner product:

$$\langle \vartheta, v\rangle_{W_2^1} = \vartheta(a)v(a) + \int_a^b \vartheta'(\xi)v'(\xi)d\xi \tag{8}$$

and the norm:

$$\|\vartheta\|_{W_2^1} = \sqrt{\langle \vartheta, \vartheta\rangle_{W_2^1}},\ where \vartheta, \mathrm{v} \in \mathrm{W}_2^1[\mathrm{a, b}]. \tag{9}$$

Definition 2.2.3 The function space $W_2^2[a, b]$ is defined by:

$W_2^2[a, b] = \{\vartheta | \vartheta, \vartheta' are\ absolutely\ continuous\ functions\ and\ \vartheta'' \in L^2[a, b], \vartheta(a) = 0\}$, with the inner product:

$$\langle \vartheta, v\rangle_{W_2^2} = \vartheta(a)v(a) + \vartheta(b)v(b) + \int_a^b \vartheta''(\xi)v''(\xi)d\xi \tag{10}$$

and the norm:

$$\|\vartheta\|_{W_2^2} = \sqrt{\langle \vartheta, \vartheta\rangle_{W_2^2}},\ where\ \vartheta, v \in \mathrm{W}_2^2[\mathrm{a, b}]. \tag{11}$$

Definition 2.2.4 The function space $W_2^3[a, b]$ is defined by:

$$W_2^3[a, b] = \left\{\vartheta | \vartheta,\ \vartheta',\ \vartheta''\ are\ absolutely\ continuous\ functions\ and\ \vartheta''' \in L^2[a, b]\ \ \vartheta(a) = \vartheta'(a) = 0\right\},$$

with the inner product:

$$\langle \vartheta, v\rangle_{W_2^3} = \vartheta(a)v(a) + \vartheta'(a)v'(a) + \vartheta''(a)v''(a) + \int_a^b \vartheta'''(\xi)v'''(\xi)d\xi \tag{12}$$

and the norm:

$$\|\vartheta\|_{W_2^3} = \sqrt{\langle \vartheta, \vartheta\rangle_{W_2^3}},\ where \vartheta, \mathrm{v} \in \mathrm{W}_2^3[\mathrm{a, b}]. \tag{13}$$

Theorem 2.2.1 *The space $W_2^3[a, b]$ is a complete reproducing kernel space and its reproducing kernel function $\grave{O}_\xi$ is given by.*

$$\mathcal{Q}_\xi(\eta) = \mathcal{Q}(\xi, \eta) = \begin{cases} q_1(\xi, \eta), & a \le \eta \le \xi \le b, \\ q_1(\eta, \xi), & a \le \xi < \eta \le b. \end{cases} \tag{14}$$

where:

$$q_1(\xi, \eta) = \frac{-1}{120}(a-\eta)^2\big(6a^3 - 3a^2(5\xi + \eta + 10) + 2a\big(5\xi^2 + 5\xi(\eta + 6) - \eta^2\big) - 10\xi^2(\eta + 3) + 5\xi\eta^2 - \eta^3\big).$$

Definition 2.2.5 The function space $W_2^3[a, b]$ is defined by:

$\bar{W}_2^3[a, b] = \big\{\vartheta | \vartheta,\ \vartheta',\ \vartheta''$ *are absolutely continuous functions and* $\vartheta''' \in L^2[a, b],\ \vartheta(a) = \vartheta(b) = 0\big\}$ with the inner product:

$$\langle \vartheta, v\rangle_{\bar{W}_2^3} = \vartheta(a)v(a) + \vartheta'(a)v'(a) + \vartheta(b)v(b) + \int_a^b \vartheta'''(\xi)v'''(\xi)d\xi \tag{15}$$

and the norm:

$$\|\vartheta\|_{\overline{W}_2^3} = \sqrt{\langle \vartheta, \vartheta\rangle_{\overline{W}_2^3}},\ where \vartheta,\ \mathrm{v} \in \overline{\mathrm{W}}_2^3[\mathrm{a, b}]. \tag{16}$$

Theorem 2.2.2 *The space $\overline{W}_2^3[a, b]$ is a complete reproducing kernel space and its reproducing kernel function $\overline{\grave{O}}_\xi$ is given by.*

$$\grave{O}_\xi(\eta) = \bar{\grave{O}}(\xi, \eta) = \begin{cases} q_2(\xi, \eta), & a \le \eta \le \xi \le b, \\ q_2(\eta, \xi), & a \le \xi < \eta \le b. \end{cases} \tag{17}$$

where

$$\begin{aligned} q_2(\xi, \eta) = {} & \frac{1}{120(a-b)^2}(a-\eta)(-4a^4(b-\xi)(b-\eta) - 6b^3\xi^2\eta + a^3(b-\xi)(b-\eta)(6b + 7\xi + 3\eta) \\ & + \xi^2\eta\big(-120 + \xi^3 + \eta^3\big) - 3a^2(b-\eta)(\xi\eta(-3\xi + \eta) + 2b^2(2\xi + \eta) - b(4\xi^2 - \xi\eta + \eta^2)) \\ & - 5b\xi\big(-24\eta + \xi^3\eta + \xi\big(-24 + \eta^3\big)\big) + b^2\big(10\xi^3\eta - \eta^4 + 5\xi\big(-24 + \eta^3\big)\big) + a(6b^3\xi(\xi + 2\eta) \\ & - b^2\big(-120 + 10\xi^3 + 12\xi^2\eta + 15\xi\eta^2 + \eta^3\big) + \xi\big(-\xi^4 + \xi\eta^3 - 2\eta\big(-60 + \eta^3\big)\big) \\ & + b\big(-120\xi + 5\xi^4 + 15\xi^2\eta^2 + 2\eta\big(-60 + \eta^3\big)\big)) \end{aligned} \tag{18}$$

Proof By definition 2.2.5, we have

$$\begin{aligned} & \bar{\vartheta}_1(\xi) - \sum_{k=0}^{1} \frac{\bar{\vartheta}_1^{(k)}(0)}{k!}(\xi - 0)^k + y_1\frac{1}{\Gamma(\alpha)}\int_0^\xi (\xi - t)^{\alpha-1}\bar{\vartheta}_1(t)dt \\ & = \frac{1}{\Gamma(\alpha)}\int_0^\xi (\xi - t)^{\alpha-1}\bar{f}_1(t)dt. \end{aligned}$$

then by applying the integration by parts three times for the third scheme of the right-hand, we obtain

$$\left\langle \vartheta,\ \grave{O}_\xi \right\rangle_{W_2^3} = \vartheta(a)\grave{O}_\xi(a) + \vartheta'(a)\grave{O}_\xi'(a) + \vartheta(b)\grave{O}_\xi(b)$$

$$+\vartheta''(b)\grave{O}_\xi'''(b)-\vartheta''(a)\grave{O}_\xi'''(a)-\vartheta'(b)\grave{O}_\xi^{(4)}(b)+\vartheta'(a)\grave{O}_\xi^{(4)}(a)$$
$$+\vartheta(b)\grave{O}_\xi^{(5)}(b)-\vartheta(a)\grave{O}_\xi^{(5)}(a)-\int_a^b\vartheta(\eta)\grave{O}_\xi^{(6)}(\eta)d\eta.$$

Note that the reproducing property is $\left\langle\vartheta(\eta),\ \grave{O}_\xi(\eta)\right\rangle_{\overline{W}_2^3}=\vartheta(\xi),$

Since $\vartheta(\eta),\ \grave{O}_\xi(\eta)\in\overline{W}_2^3[a,\,b]$, we have.

(1) $\grave{O}_\xi(a)-\grave{O}_\xi^{(5)}(a)=0,$
(2) $\grave{O}_\xi'(a)+\grave{O}_\xi^{(4)}(a)=0,$
(3) $\grave{O}_\xi(b)+O@_\xi^{(5)}(b)=0,$
(4) $\grave{O}_\xi'''(b)=0,$
(5) $\grave{O}_\xi'''(a)=0,$
(6) $\grave{O}_\xi^{(4)}(b)=0.$

Thus, we need to solve the BVP $-\grave{O}_\xi^{(6)}(\eta)=\delta(\xi-\eta)$ subject to the conditions (1–6).
When $\xi\neq\eta$, we know $\grave{O}_\xi^{(6)}(\eta)=0$.
Consequently, we attain

$$\grave{O}_\xi(\eta)=\begin{cases}\sum\limits_{j=0}^{5}c_j(\xi)\eta^j,\ a\le\eta\le\xi\le b,\\ \sum\limits_{j=0}^{5}d_j(\xi)\eta^j,\ a\le\xi<\eta\le b.\end{cases}$$

Since $\grave{O}_\xi^{(6)}(\eta)=\delta(\xi-\eta)$, we have $\grave{O}_{\xi^+}^{(k)}(\xi)=\grave{O}_{\xi^-}^{(k)}(\xi)$, $k=0,\,1,\,2,\,3,\,4,$ $\grave{O}_{\xi^+}^{(5)}(\xi)-\grave{O}_{\xi^-}^{(5)}(\xi)=-1$.

The unknown coefficients $c_j(\xi)$ and $d_j(\xi)(j=0,\,1,\,2,\,3,\,4,\,5)$ can be found by using Mathematica 12, hence (18) is obtained.

Solution of Problem (1)

In this section, we consider the 1-D fractional interface problem (1) with the interface conditions (2). We solve the problem (1) on intervals (0, z) and (z, 1) by using the shooting method and RKHSs, respectively.

Now we apply the shooting method to (1) then we have

$$\begin{cases}D^\alpha\vartheta(\xi)+A(\xi)\vartheta(\xi)=f(\xi),\ \xi\in(0,z)\cup(z,1),\\ \vartheta(0)=\beta_0,\vartheta'(0)=\beta_1,\\ \vartheta(z^+)=x_1\vartheta(z^-)+\gamma_0,\vartheta'(z^+)=x_2\vartheta'(z^-)+\gamma_1.\end{cases}\tag{19}$$

On (0, z), we get

$$D^\alpha\vartheta_1(\xi)+y_1\vartheta_1(\xi)=f_1(\xi),\ \vartheta_1(0)=\beta_0,\ \vartheta_1'(0)=\sigma_1.\tag{20}$$

We discuss Eq. (20) with homogeneous conditions, that is,

$$D^\alpha\overline{\vartheta}_1(\xi)+y_1\overline{\vartheta}_1(\xi)=\overline{f}_1(\xi),\ \overline{\vartheta}_1(0)=0,\ \overline{\vartheta}_1'(0)=0.\tag{21}$$

where
$\vartheta_1(\xi) = \overline{\vartheta}_1(\xi) + \delta_1(\xi)$, $\overline{f}_1(\xi) = f_1(\xi) - L\delta_1(\xi)$ and $\delta_1(\xi) = \beta_0 + \sigma_1\xi$.

By applying the Riemann–Liouville fractional integral operator of the order α of both sides of Eq. (21), we have

$$\overline{\vartheta}_1(\xi) - \sum_{k=0}^{1} \frac{\overline{\vartheta}_1^{(k)}(0)}{k!}(\xi - 0)^k + y_1 \frac{1}{\Gamma(\alpha)} \int_0^{\xi} (\xi - t)^{\alpha-1}\overline{\vartheta}_1(t)dt = \frac{1}{\Gamma(\alpha)} \int_0^{\xi} (\xi - t)^{\alpha-1}\overline{f}_1(t)dt. \tag{22}$$

But since $\overline{\vartheta}_1^{(j)}(0) = 0,\ j = 0,\ 1$ then we have

$$\overline{\vartheta}_1(\xi) = \overline{F}_1\big(\xi,\ \overline{\vartheta}_1(\xi)\big) \tag{23}$$

where $\overline{F}_1\big(\xi,\ \overline{\vartheta}_1(\xi)\big) = \frac{1}{\Gamma(\alpha)} \int_0^{\xi}(\xi - t)^{\alpha-1}\overline{f}_1(t)dt - \mathrm{y}_1 \frac{1}{\Gamma(\alpha)} \int_0^{\xi}(\xi - \mathrm{t})^{\alpha-1}\overline{\vartheta}_1(\mathrm{t})\mathrm{dt}$.

Choose a countable dense subset $\{\xi_1,\ \xi_2,\ \ldots,\ \xi_N\}$ in $(0,\ z)$, we define

$$\psi_j(\xi) = \grave{O}(\xi,\ \eta)\Big|_{\eta=\xi_j},\ j = 1,\ 2,\ \ldots,\ N. \tag{24}$$

The solution of (21) can be written as

$$\overline{\vartheta}_{1,N}(\xi) = \sum_{j=1}^{N} d_j \psi_j(\xi), \tag{25}$$

where $\{d_j\}_{j=1}^{N}$ are constants to be determined. Therefore, the solution of (21) is given by

$$\vartheta_{1,N}(\xi) = \overline{\vartheta}_{1,N}(\xi) + \delta_1(\xi). \tag{26}$$

Because of the uniformed convergence of $\vartheta_{1,N}(\xi)$ and its derivative, utilizing those states in the interface point, $\vartheta_{1,N}(\xi)$ could provide an exact close estimation of the values of $\vartheta\left(z^+\right)$, $\vartheta'\left(z^+\right)$.

Now the problem (19) on (z, 1) can be written as

$$\begin{cases} D^{\alpha}\vartheta_2(\xi) + y_2\vartheta_2(\xi) = f_2(\xi)\ , \\ \vartheta_2(z) = x_1\vartheta_{1,N}\left(z^-\right) + \gamma_0,\ \ \vartheta_2'(z) = x_2\vartheta_{1,N}'\left(z^-\right) + \gamma_1\ . \end{cases} \tag{27}$$

Toward utilizing the manner for solving the problem (20), we get $\vartheta_{2,N}(\xi)$ to the problem (19) on $(z,\ 1)$. So we have an approximate solution to the problem (19), which is given by

$$\vartheta_N(\xi) = \begin{cases} \vartheta_{1,N}(\xi)\xi \in (0,\ z), \\ \vartheta_{2,N}(\xi)\xi \in (z,\ 1). \end{cases} \tag{28}$$

Applications

In this part, we introduce some applications to solve 1-D interface problems of fractional order.

Example 1 Consider the following problem [8]:

$$\gamma D^{\alpha}\vartheta(\xi) = 12\xi^2,\ \gamma = \begin{cases} 1,\ \xi \in \left(0,\ \frac{1}{2}\right),\ \alpha \in (1,\ 2]. \\ 2,\ \xi \in \left(\frac{1}{2},\ 1\right), \end{cases}$$

subject to the boundary and interface conditions:

$$\vartheta(0) = 0,\ \vartheta(1) = \frac{17}{32},\ \vartheta\left(\frac{1}{2}^{+}\right) = \vartheta\left(\frac{1}{2}^{-}\right),\ \vartheta'\left(\frac{1}{2}^{+}\right) = \vartheta'\left(\frac{1}{2}^{-}\right).$$

As $\alpha = 2$, the exact solution is

$$\vartheta(\xi) = \begin{cases} \xi^4,\ \xi \in \left(0,\ \frac{1}{2}\right). \\ \frac{1}{2}\left(\xi^4 + \frac{1}{16}\right),\ \xi \in \left(\frac{1}{2},\ 1\right). \end{cases}$$

After the initial conditions have been homogenized, choose.

$$\xi_j = \begin{cases} \frac{j}{2N},\ \xi \in \left(0,\ \frac{1}{2}\right), \\ \frac{1}{2} + \frac{j-1}{2(N-1)},\ \xi \in \left(\frac{1}{2},\ 1\right), \end{cases}\ for j = 1,\ 2,\ \ldots,\ N.$$

Then we apply the RKHS method with $N = 50$, Table 1 which describes the exact and approximate solutions of $\vartheta(\xi)$ for $\alpha = 2$ and approximate solutions for different values of α.

The graph in Fig. 1a represents the exact and approximate solution $\vartheta(\xi)$ when $\alpha = 2$. In Fig. 1b, graphs of the approximate solutions of $\vartheta(\xi)$ are plotted for different values of α. It is clear from Fig. 1b that the approximate solutions are insensible arrangements with the exact solution when $\alpha = 2$, and the solutions are continuously based on a fractional derivative. The graph in Fig. 1c represents the absolute errors of $\vartheta(\xi)$ when $\alpha = 2$.

Example 2 Consider the following problem [8]:

$$\gamma D^{\alpha}\vartheta(\xi) = 56\xi^6,\ \gamma = \begin{cases} 1,\ \xi \in \left(0,\ \frac{1}{2}\right),\ \alpha \in (1,\ 2]. \\ 2,\ \xi \in \left(\frac{1}{2},\ 1\right), \end{cases}$$

Table 1 Numerical results for $\vartheta(\xi)$ in Example 1

ξ	Exact solutions $\alpha = 2$	Approximate solutions				Absolute error $\alpha = 2$
		$\alpha = 2$	$\alpha = 1.9$	$\alpha = 1.8$	$\alpha = 1.7$	
0.1	0.0001	0.0001	0.00017	0.00023	0.00033	5.33167×10^{-7}
0.2	0.0016	0.00160	0.00224	0.00301	0.00406	1.85062×10^{-6}
0.3	0.0081	0.00810	0.01071	0.01393	0.01813	3.94932×10^{-6}
0.4	0.0256	0.02561	0.03273	0.04147	0.05248	6.82927×10^{-6}
0.5	0.0625	0.06251	0.07801	0.09674	0.11977	1.04000×10^{-5}
0.6	0.09605	0.09606	0.10644	0.12009	0.13889	7.61874×10^{-6}
0.7	0.1513	0.15131	0.15429	0.15911	0.16732	5.12922×10^{-6}
0.8	0.23605	0.23605	0.23431	0.23340	0.23450	3.02654×10^{-6}
0.9	0.3593	0.35930	0.35632	0.35359	0.35176	1.31528×10^{-6}
1	0	0	0	0	0	0

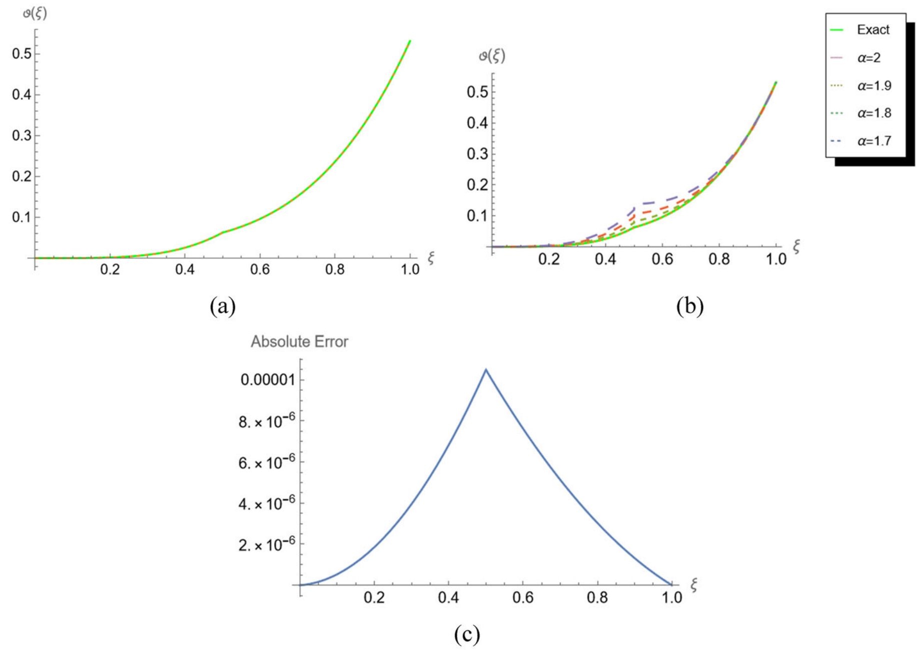

Fig. 1 Solution and graphical results of Example 1

subject to the boundary and interface conditions:

$$\vartheta(0) = -1,\ \vartheta(1) = \frac{769}{512},\ \vartheta\left(\frac{1}{2}^{+}\right) = \vartheta\left(\frac{1}{2}^{-}\right) + 2,\ \vartheta'\left(\frac{1}{2}^{+}\right) = \frac{1}{2}\vartheta'\left(\frac{1}{2}^{-}\right).$$

As $\alpha = 2$, the exact solution is.

$$\vartheta(\xi) = \begin{cases} \xi^8 - 1,\ \xi \in \left(0,\ \frac{1}{2}\right). \\ \frac{1}{2}\left(\xi^8 + \frac{1}{256}\right),\ \xi \in \left(\frac{1}{2},\ 1\right). \end{cases}$$

After the initial conditions have been homogenized, choose

$$\xi_j = \begin{cases} \frac{j}{2N},\ \xi \in \left(0,\ \frac{1}{2}\right), \\ \frac{1}{2} + \frac{j-1}{2(N-1)},\ \xi \in \left(\frac{1}{2},\ 1\right), \end{cases} \text{for} j = 1, 2, \ldots, N.$$

Then we apply the RKHS method with $N = 50$, Table 2 which describes the exact and approximate solutions of $\vartheta(\xi)$ for $\alpha = 2$ and approximate solutions for different values of α.

The graph in Fig. 2a represents the exact and approximate solution $\vartheta(\xi)$ when $\alpha = 2$. In Fig. 2b, graphs of the approximate solutions of $\vartheta(\xi)$ are plotted for different values of α. It is clear from Fig. 2b that the approximate solutions are insensible arrangements with the exact solution when $\alpha = 2$, and the solutions are continuously based on a fractional derivative. The graph in Fig. 2c represents the absolute errors of $\vartheta(\xi)$ when $\alpha = 2$.

Example 3 Consider the following problem:

$$\gamma D^{\alpha}\vartheta(\xi) = \begin{cases} e^{\xi},\ \xi \in \left(0,\ \frac{1}{2}\right) \\ sec^2\left(\xi - \frac{1}{2}\right)\tan\left(\xi - \frac{1}{2}\right),\ \xi \in \left(\frac{1}{2},\ 1\right) \end{cases},\ \gamma = \begin{cases} 1,\ \xi \in \left(0,\ \frac{1}{2}\right),\ \alpha \in (1, 2]. \\ 2,\ \xi \in \left(\frac{1}{2},\ 1\right), \end{cases}$$

Table 2 Numerical results for $\vartheta(\xi)$ in Example 2

ξ	Exact solutions $\alpha = 2$	Approximate solutions				Absolute error $\alpha = 2$
		$\alpha = 2$	$\alpha = 1.9$	$\alpha = 1.8$	$\alpha = 1.7$	
0.1	−1	−1	−1	−1	−1	1.29807×10^{-10}
0.2	−0.99999	−0.99999	−0.99999	−0.99999	−0.99999	8.28191×10^{-9}
0.3	−0.99993	−0.99993	−0.99991	−0.99988	−0.99983	9.42817×10^{-8}
0.4	−0.99934	−0.99934	−0.99910	−0.99879	−0.99837	5.29630×10^{-7}
0.5	−0.99609	−0.99609	−0.99477	−0.99310	−0.99088	2.02019×10^{-6}
0.6	0.01035	0.01034	0.00665	0.00458	0.00367	9.30563×10^{-6}
0.7	0.03078	0.03076	0.00680	−0.02005	−0.05157	1.80000×10^{-5}
0.8	0.08584	0.08582	0.04844	0.00508	−0.04677	2.18000×10^{-5}
0.9	0.21719	0.21717	0.18246	0.14182	0.09309	1.75000×10^{-5}
1	0	0	0	0	0	0

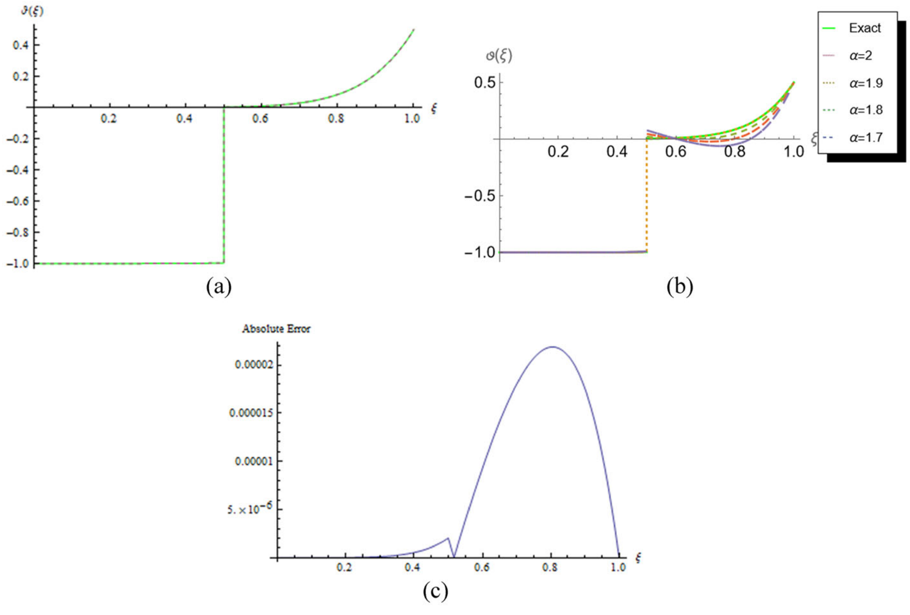

Fig. 2 Solution and graphical results of Example 2

subject to the boundary and interface conditions:

$$\vartheta(0) = 1,\ \vartheta(1) = e^{\frac{1}{2}} + \tan\left(\frac{1}{2}\right),\ \vartheta\left(\frac{1}{2}^{+}\right) = \vartheta\left(\frac{1}{2}^{-}\right),\ \vartheta'\left(\frac{1}{2}^{+}\right) = e^{-\frac{1}{2}}\vartheta'\left(\frac{1}{2}^{-}\right).$$

As $\alpha = 2$, the exact solution is $\vartheta(\xi) = \begin{cases} e^{\xi}, & \xi \in \left(0, \frac{1}{2}\right). \\ e^{\frac{1}{2}} + \tan\left(\xi - \frac{1}{2}\right), & \xi \in \left(\frac{1}{2}, 1\right). \end{cases}$

After the initial conditions have been homogenized, choose

$$\xi_j = \begin{cases} \frac{j}{2N}, \xi \in \left(0, \frac{1}{2}\right), \\ \frac{1}{2} + \frac{j-1}{2(N-1)}, \xi \in \left(\frac{1}{2}, 1\right), \end{cases} \text{for} j = 1, 2, \ldots, N.$$

Then we apply the RKHS method with $N = 50$, Table 3 which describes the exact and approximate solutions of $\vartheta(\xi)$ for $\alpha = 2$ and approximate solutions for different values of α.

The graph in Fig. 3a represents the exact and approximate solution $\vartheta(\xi)$ when $\alpha = 2$. In Fig. 3b, graphs of the approximate solutions of $\vartheta(\xi)$ are plotted for different values of α. It is clear from Fig. 3b that the approximate solutions are insensible arrangements with the exact solution when $\alpha = 2$, and the solutions are continuously based on a fractional derivative. The graph in Fig. 3c represents the absolute errors of $\vartheta(\xi)$ when $\alpha = 2$.

Example 4 Consider the following problem:

$$\gamma D^{\alpha}\vartheta(\xi) = \begin{cases} \sin(\pi\xi), & \xi \in \left(0, \frac{1}{2}\right) \\ \left(\xi - \frac{1}{2}\right), & \xi \in \left(\frac{1}{2}, 1\right) \end{cases}, \quad \gamma = \begin{cases} -\pi^2, & \xi \in \left(0, \frac{1}{2}\right), \ \alpha \in (1, 2]. \\ 6, & \xi \in \left(\frac{1}{2}, 1\right), \end{cases}$$

subject to the boundary and interface conditions:

$$\vartheta(0) = 1, \ \vartheta(1) = \frac{9}{8}, \ \vartheta\left(\frac{1}{2}^{+}\right) = \vartheta\left(\frac{1}{2}^{-}\right), \ \vartheta'\left(\frac{1}{2}^{+}\right) = \vartheta'\left(\frac{1}{2}^{-}\right).$$

As $\alpha = 2$, the exact solution is.

$$\vartheta(\xi) = \begin{cases} \sin(\pi\xi), & \xi \in \left(0, \frac{1}{2}\right). \\ \left(\xi - \frac{1}{2}\right)^3 + 1, & \xi \in \left(\frac{1}{2}, 1\right). \end{cases}$$

After the initial conditions have been homogenized, choose

$$\xi_j = \begin{cases} \frac{j}{2N}, & \xi \in \left(0, \frac{1}{2}\right), \\ \frac{1}{2} + \frac{j-1}{2(N-1)}, & \xi \in \left(\frac{1}{2}, 1\right), \end{cases} \text{for } j = 1, 2, \ldots, N.$$

Table 3 Numerical results for $\vartheta(\xi)$ in Example 3

ξ	Exact solutions $\alpha = 2$	Approximate solutions				Absolute error $\alpha = 2$
		$\alpha = 2$	$\alpha = 1.9$	$\alpha = 1.8$	$\alpha = 1.7$	
0.1	1.10517	1.10517	1.10688	1.10920	1.11236	1.38358×10^{-8}
0.2	1.22140	1.22140	1.22709	1.23434	1.24352	5.07672×10^{-8}
0.3	1.34986	1.34986	1.36106	1.37476	1.39140	1.13166×10^{-7}
0.4	1.49182	1.49183	1.50976	1.53103	1.55611	2.03710×10^{-7}
0.5	1.64872	1.64872	1.67439	1.70415	1.73841	3.25359×10^{-7}
0.6	1.74906	1.74906	1.76891	1.79239	1.82031	9.03652×10^{-8}
0.7	1.85143	1.85143	1.86473	1.88056	1.89956	1.10708×10^{-7}
0.8	1.95806	1.95806	1.96564	1.97479	1.98595	2.35579×10^{-7}
0.9	2.07151	2.07151	2.07455	2.07829	2.08299	2.27158×10^{-7}
1	0	0	0	0	0	0

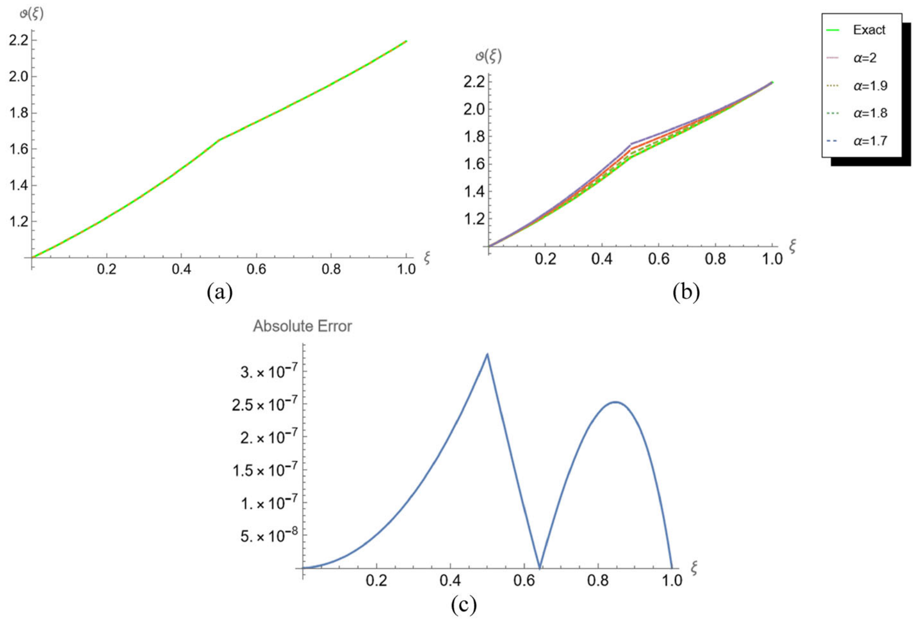

Fig. 3 Solution and graphical results of Example 3

Then we apply the RKHS method with $N = 50$, Table 4 which describes the exact and approximate solutions of $\vartheta(\xi)$ for $\alpha = 2$ and approximate solutions for different values of α.

The graph in Fig. 4a represents the exact and approximate solution $\vartheta(\xi)$ when $\alpha = 2$. In Fig. 4b, graphs of the approximate solutions of $\vartheta(\xi)$ are plotted for different values of α. It is clear from Fig. 4b that the approximate solutions are insensible arrangements with the exact

Table 4 Numerical results for $\vartheta(\xi)$ in Example 4

ξ	Exact solutions $\alpha = 2$	Approximate solutions				Absolute error $\alpha = 2$
		$\alpha = 2$	$\alpha = 1.9$	$\alpha = 1.8$	$\alpha = 1.7$	
0.1	0.30902	0.30898	0.30544	0.30241	0.29811	3.78149×10^{-5}
0.2	0.58779	0.58771	0.57177	0.55457	0.53193	7.56505×10^{-5}
0.3	0.80902	0.80890	0.76850	0.72305	0.66592	1.12303×10^{-4}
0.4	0.95106	0.95091	0.87385	0.78694	0.68136	1.47327×10^{-4}
0.5	1.	0.99982	0.87615	0.73797	0.57483	1.80438×10^{-4}
0.6	1.00100	1.00086	0.89998	0.78850	0.65951	1.44344×10^{-4}
0.7	1.00800	1.00789	0.92826	0.84032	0.73906	1.08254×10^{-4}
0.8	1.02700	1.02693	0.97092	0.90920	0.83856	7.21676×10^{-5}
0.9	1.06400	1.06396	1.03442	1.00196	0.96509	3.60833×10^{-5}
1	0	0	0	0	0	0

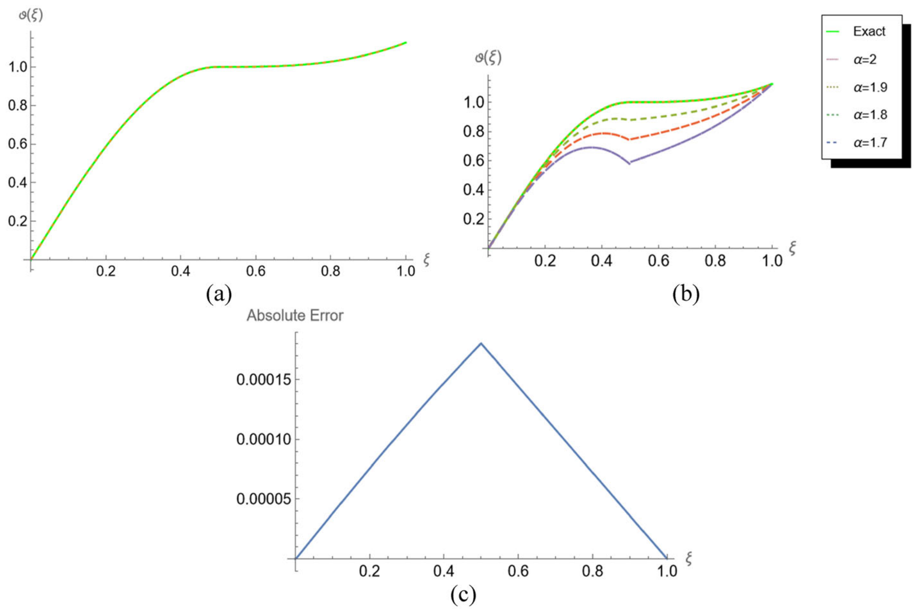

Fig. 4 Solution and graphical results of Example 4

solution when $\alpha = 2$, and the solutions are continuously based on a fractional derivative. The graph in Fig. 4c represents the absolute errors of $\vartheta(\xi)$ when $\alpha = 2$.

Example 5 Consider the following problem [8]:

$$\rho(\xi) D^{\alpha} \vartheta(\xi) + \rho'(\xi) \vartheta^{'(\xi)} - \sigma(\xi) \vartheta(\xi) = \mathcal{F}(\xi), \, \xi \in \left(0, \frac{1}{2}\right) \cup \left(\frac{1}{2}, 1\right) \alpha \in (1, 2].$$

where:

$$\rho(\xi) = \begin{cases} 3e^{-10\xi^4\left(\xi-\frac{1}{2}\right)^4}, \xi \in \left(0, \frac{1}{2}\right) \\ 3, \xi \in \left(\frac{1}{2}, 1\right) \end{cases}, \, \sigma(\xi) = \begin{cases} 2, \xi \in \left(0, \frac{1}{2}\right). \\ 1, \xi \in \left(\frac{1}{2}, 1\right). \end{cases}$$

subject to the boundary and interface conditions:

$$\vartheta(0) = 0, \, \vartheta(1) = 1.0156, \, \vartheta\left(\frac{1}{2}^{+}\right) = \vartheta\left(\frac{1}{2}^{-}\right), \, \vartheta'\left(\frac{1}{2}^{+}\right) = \vartheta'\left(\frac{1}{2}^{-}\right).$$

As $\alpha = 2$ and $\mathcal{F}(\xi)$ is selected such that its exact solution is.

$$\vartheta(\xi) = \begin{cases} \sin(\pi\xi), & \xi \in \left(0, \frac{1}{2}\right). \\ 2\left(\xi - \frac{1}{2}\right)^7 + 1, & \xi \in \left(\frac{1}{2}, 1\right). \end{cases}$$

After the initial conditions have been homogenized, choose

$$\xi_j = \begin{cases} \frac{j}{2N}, \xi \in \left(0, \frac{1}{2}\right), \\ \frac{1}{2} + \frac{j}{2N}, \xi \in \left(\frac{1}{2}, 1\right), \end{cases} \text{ for } j = 1, 2, \ldots, N.$$

Then we apply the RKHS method with $N = 50$, Table 5 which describes the exact and

Table 5 Numerical results for $\vartheta(\xi)$ in Example 5

ξ	Exact solutions $\alpha = 2$	Approximate solutions				Absolute error $\alpha = 2$
		$\alpha = 2$	$\alpha = 1.9$	$\alpha = 1.8$	$\alpha = 1.7$	
0.1	0.30902	0.30902	0.30544	0.30240	0.29809	1.80263×10^{-6}
0.2	0.58779	0.58776	0.57169	0.55441	0.53161	2.51361×10^{-5}
0.3	0.80902	0.80895	0.76818	0.72232	0.66441	6.88451×10^{-5}
0.4	0.95106	0.95097	0.87298	0.78478	0.67688	8.99297×10^{-5}
0.5	1.	0.99991	0.87412	0.73278	0.56422	8.75012×10^{-5}
0.6	1.	1.	0.90608	0.79344	0.65916	1.78911×10^{-9}
0.7	1.00003	1.00003	0.93331	0.84733	0.74470	5.71650×10^{-8}
0.8	1.00044	1.00044	0.95775	0.89856	0.82775	4.34177×10^{-7}
0.9	1.00328	1.00328	0.98214	0.95076	0.91308	1.83051×10^{-6}
1	0	0	0	0	0	0

approximate solutions of $\vartheta(\xi)$ for $\alpha = 2$ and approximate solutions for different values of α.

The graph in Fig. 5a represents the exact and approximate solution $\vartheta(\xi)$ when $\alpha = 2$. In Fig. 5b, graphs of the approximate solutions of $\vartheta(\xi)$ are plotted for different values of α. It is clear from Fig. 5b that the approximate solutions are insensible arrangements with the exact

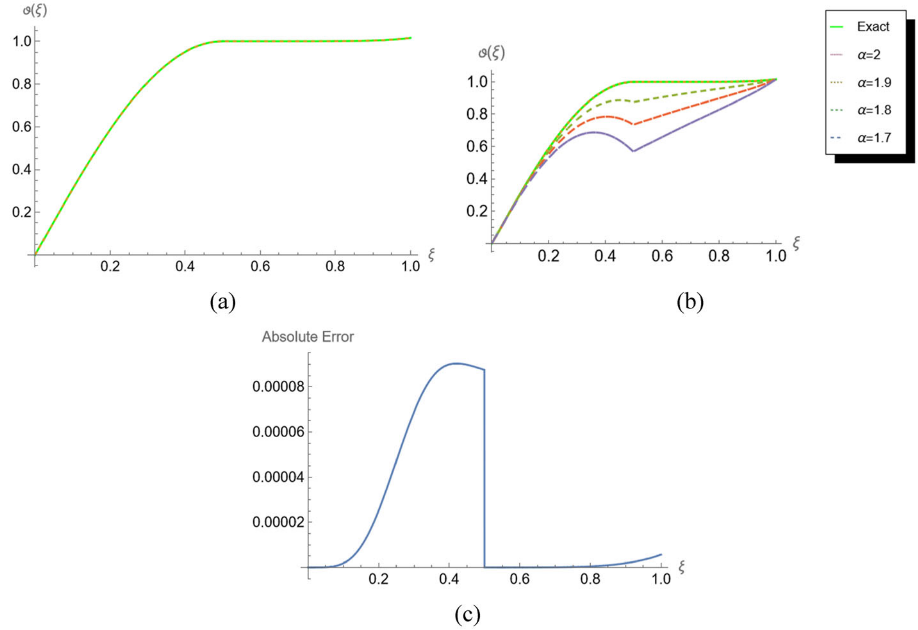

Fig. 5 Solution and graphical results of Example 5

solution when $\alpha = 2$, and the solutions are continuously based on a fractional derivative. The graph in Fig. 5c represents the absolute errors of $\vartheta(\xi)$ when $\alpha = 2$.

Conclusion

In this paper, a numerical method has been employed for solving 1-D interface problems of fractional order in the Caputo sense. The key to the solution procedure is the combination of the reproducing kernel functions and the shooting method. The main advantage of the method is its fast convergence to the solution. In practice, the utilization of the method is straightforward if some symbolic software such as Mathematica is used to implement the calculations. The results of examples illustrate the reliability and consistency of the method. Moreover, the solutions obtained are easily programmable approximants to the analytic solutions of the original problems with the accuracy required.

Funding No funding was received to assist with the preparation of this manuscript.

Data Availability Data sharing is not applicable to this article as no datasets were generated or analyzed during the current study.

Declarations

Conflict of interest The authors declare that they have no known competing financial interests or personal relationships that could have appeared to influence the work reported in this paper.

References

1. Pesin, Y.B.: Dimension theory in dynamical systems: contemporary views and applications. Ergod. Theory Dyn. Syst. **18**(4), 1043–1045 (1998). https://doi.org/10.1017/S0143385798128298
2. Layton, A.T.: Using integral equations and the immersed interface method to solve immersed boundary problems with stiff forces. Comput. Fluids **38**(2), 266–272 (2009). https://doi.org/10.1016/j.compfluid.2008.02.003
3. Hadley, G.R.: High-accuracy finite-difference equations for dielectric waveguide analysis I: uniform regions and dielectric interfaces. J. Lightwave Technol. **20**(7), 1210–1218 (2002). https://doi.org/10.1109/JLT.2002.800361
4. Zhao, S.: High order matched interface and boundary methods for the Helmholtz equation in media with arbitrarily curved interfaces. J. Comput. Phys. **229**(9), 3155–3170 (2010). https://doi.org/10.1016/j.jcp.2009.12.034
5. Hou, T.Y., Li, Z., Osher, S., Zhao, H.: A hybrid method for moving interface problems with application to the Hele-Shaw flow. J. Comput. Phys. **134**(2), 236–252 (1997). https://doi.org/10.1006/jcph.1997.5689
6. Horikis, T.P., Kath, W.L.: Modal analysis of circular Bragg fibers with arbitrary index profiles. Opt. Lett. **31**(23), 3417 (2006). https://doi.org/10.1364/OL.31.003417
7. Gong, Y., Li, B., Li, Z.: Immersed-Interface Finite-Element methods for Elliptic Interface problems with nonhomogeneous jump conditions. SIAM J. Numer. Anal. **46**(1), 472–495 (2008). https://doi.org/10.1137/060666482
8. Xu, M., Zhao, Z., Niu, J., Guo, L., Lin, Y.: A simplified reproducing kernel method for 1-D elliptic type interface problems. J. Comput. Appl. Math. **351**, 29–40 (2019). https://doi.org/10.1016/j.cam.2018.10.027
9. Li, X.Y., Wu, B.Y.: A new kernel functions based approach for solving 1-D interface problems. Appl. Math. Comput. **380**, 125276 (2020). https://doi.org/10.1016/j.amc.2020.125276
10. Epshteyn, Y., Phippen, S.: High-order difference potentials methods for 1D elliptic type models. Appl. Numer. Math. **93**, 69–86 (2015). https://doi.org/10.1016/j.apnum.2014.02.005

11. Ray, S.S., Atangana, A., Noutchie, S.C.O., Kurulay, M., Bildik, N., Kilicman, A.: Fractional calculus and its applications in applied mathematics and other sciences. Math. Probl. Eng. **2014**, 1–2 (2014). https://doi.org/10.1155/2014/849395
12. Baleanu, D., Mohammadi, H., Rezapour, S.: A mathematical theoretical study of a particular system of Caputo-Fabrizio fractional differential equations for the Rubella disease model. Adv. Differ. Equ. **2020**(1), 184 (2020). https://doi.org/10.1186/s13662-020-02614-z
13. Alqahtani, R.T., Ahmad, S., Akgül, A.: Mathematical analysis of Biodegradation model under nonlocal operator in Caputo sense. Mathematics **9**(21), 2787 (2021). https://doi.org/10.3390/math9212787
14. Johansyah, M.D., Supriatna, A.K., Rusyaman, E., Saputra, J.: Application of fractional differential equation in economic growth model: a systematic review approach. AIMS Math. **6**(9), 10266–10280 (2021). https://doi.org/10.3934/math.2021594
15. Bazhlekov, I., Bazhlekova, E.: Fractional derivative modeling of bioreaction-diffusion processes. In: AIP Conference Proceedings, p. 060006 (2021), https://doi.org/10.1063/5.0041611
16. Zhang, L., Rahman, M.U., Ahmad, S., Riaz, M.B., Jarad, F.: Dynamics of fractional order delay model of coronavirus disease. AIMS Math. **7**(3), 4211–4232 (2022). https://doi.org/10.3934/math.2022234
17. Nisar, K.S., Ahmad, S., Ullah, A., Shah, K., Alrabaiah, H., Arfan, M.: Mathematical analysis of SIRD model of COVID-19 with Caputo fractional derivative based on real data. Res. Phys. **21**, 103772 (2021). https://doi.org/10.1016/j.rinp.2020.103772
18. Ahmad, S., Ullah, A., Akgül, A., Jarad, F.: A hybrid analytical technique for solving nonlinear fractional order PDEs of power law kernel: application to KdV and Fornberg-Witham equations. AIMS Math. **7**(5), 9389–9404 (2022). https://doi.org/10.3934/math.2022521
19. Beghami, W., Maayah, B., Bushnaq, S., Arqub, O.A.: The Laplace optimized decomposition method for solving systems of partial differential equations of fractional order. Int. J. Appl. Comput. Math. **8**(2), 52 (2022). https://doi.org/10.1007/s40819-022-01256-x
20. Ahmad, S., Ullah, A., Akgül, A., De la Sen, M.: A novel homotopy perturbation method with applications to nonlinear fractional order KdV and Burger equation with Exponential-Decay kernel. J. Funct. Spaces **2021**, 1–11 (2021). https://doi.org/10.1155/2021/8770488
21. Ahmad, S., Ullah, A., Akgül, A., la Sen, M.D.: A study of fractional order Ambartsumian equation involving exponential decay kernel. AIMS Math. **6**(9), 9981–9997 (2021). https://doi.org/10.3934/math.2021580
22. Ahmad, S., Ullah, A., Shah, K., Akgül, A.: Computational analysis of the third order dispersive fractional PDE under exponential-decay and Mittag-Leffler type kernels. Numer. Methods Partial Differ. Equ. 22627 (2020),https://doi.org/10.1002/num.22627.
23. Ahmad, S., Ullah, A., Arfan, M., Shah, K.: On analysis of the fractional mathematical model of rotavirus epidemic with the effects of breastfeeding and vaccination under Atangana-Baleanu (AB) derivative. Chaos Solitons Fractals **140**, 110233 (2020). https://doi.org/10.1016/j.chaos.2020.110233
24. Ullah, A., Abdeljawad, T., Ahmad, S., Shah, K.: Study of a fractional-order epidemic model of childhood diseases. J. Funct. Spaces **2020**, 1–8 (2020). https://doi.org/10.1155/2020/5895310
25. Laoubi, M., Odibat, Z., Maayah, B.: A Legendre-based approach of the optimized decomposition method for solving nonlinear Caputo-type fractional differential equations. Math. Methods Appl. Sci. (2022). https://doi.org/10.1002/mma.8237
26. Arqub, O.A., Maayah, B.: Modulation of reproducing kernel Hilbert space method for numerical solutions of Riccati and Bernoulli equations in the Atangana-Baleanu fractional sense. Chaos Solitons Fractals **125**, 163–170 (2019). https://doi.org/10.1016/j.chaos.2019.05.025
27. Maayah, B., Yousef, F., Arqub, O.A., Momani, S., Alsaedi, A.: Computing bifurcations behavior of mixed type singular time-fractional partial integrodifferential equations of Dirichlet functions types in hilbert space with error analysis. Filomat **33**(12), 3845–3853 (2019). https://doi.org/10.2298/FIL1912845M
28. Gobena, W.T., Duressa, G.F.: Parameter uniform numerical methods for singularly perturbed delay parabolic differential equations with non-local boundary condition. Int. J. Eng. Sci. Technol. **13**(2), 57–71 (2021). https://doi.org/10.4314/ijest.v13i2.7
29. Ismail, G.M., Abul-Ez, M., Zayed, M., Ahmad, H., El-Moshneb, M.: Highly accurate analytical solution for free vibrations of strongly nonlinear Duffing oscillator. J. Low Freq. Noise Vib. Act Control **41**(1), 223–229 (2022). https://doi.org/10.1177/14613484211034009
30. Berredjem, N., Maayah, B., Arqub, O.A.: A numerical method for solving conformable fractional integrodifferential systems of second-order, two-points periodic boundary conditions. Alex. Eng. J. **61**(7), 5699–5711 (2022). https://doi.org/10.1016/j.aej.2021.11.025
31. Arqub, O.A., Maayah, B.: Solutions of Bagley-Torvik and Painlevé equations of fractional order using iterative reproducing kernel algorithm with error estimates. Neural Comput. Appl. **29**(5), 1465–1479 (2018). https://doi.org/10.1007/s00521-016-2484-4

32. Arqub, O.A., Singh, J., Maayah, B., Alhodaly, M.: Reproducing kernel approach for numerical solutions of fuzzy fractional initial value problems under the Mittag-Leffler kernel differential operator. Math. Methods Appl. Sci. (2021). https://doi.org/10.1002/mma.7305
33. Arqub, O.A.: Solutions of time-fractional Tricomi and Keldysh equations of Dirichlet functions types in Hilbert space. Numer. Methods Partial Differ. Equ. **34**(5), 1759–1780 (2018). https://doi.org/10.1002/num.22236
34. Arqub, O.A., Maayah, B.: Fitted fractional reproducing kernel algorithm for the numerical solutions of ABC – Fractional Volterra integro-differential equations. Chaos Solitons Fractals **126**, 394–402 (2019). https://doi.org/10.1016/j.chaos.2019.07.023
35. Momani, S., Maayah, B., Arqub, O.A.: The reproducing kernel algorithm for numerical solution of Van Der-Pol damping model in view of the Atangana-Baleanu fractional approach. Fractals **28**(08), 2040010 (2020). https://doi.org/10.1142/S0218348X20400101
36. Arqub, O.A.: Fitted reproducing kernel Hilbert space method for the solutions of some certain classes of time-fractional partial differential equations subject to initial and Neumann boundary conditions. Comput. Math. Appl. **73**(6), 1243–1261 (2017). https://doi.org/10.1016/j.camwa.2016.11.032
37. Du, H., Shen, J.: Reproducing kernel method of solving singular integral equation with cosecant kernel. J. Math. Anal. Appl. **348**(1), 308–314 (2008). https://doi.org/10.1016/j.jmaa.2008.07.037
38. Demir, H., Baltürk, Y.: On numerical solution of fractional order boundary value problem with shooting method. ITM Web Conf. **13**, 01032 (2017). https://doi.org/10.1051/itmconf/20171301032